Biochimica et Biophysica Acta, 1153 (1993) 77–88

BBAMEM 76137

Frequency domain electrical conductivity measurements of the passive electrical properties of human lymphocytes

F. Bordi [a], C. Cametti [b,*], A. Rosi [c] and A. Calcabrini [d]

[a] *Sezione di Fisica Medica, Dipartimento di Medicina Interna, Università di Roma 'Tor Vergata', Rome (Italy),* [b] *Dipartimento di Fisica, Università di Roma 'La Sapienza', Piazzale A. Moro 5, 00185 Rome (Italy),* [c] *Laboratorio di Fisica, Istituto Superiore di Sanità, Viale Regina Elena 299, Rome (Italy) and* [d] *Laboratorio di Ultrastrutture, Istituto Superiore di Sanità – Viale Regina Elena 299, Rome (Italy)*

(Received 21 December 1992)

Key words: Electrical conductivity; Lymphocyte; Fractal model; Surface polarization; Membrane surface roughness; Conductometric property; (Human)

An extensive set of electrical conductivity measurements of human lymphocyte suspensions has been carried out in the frequency range from 1 kHz to 100 MHz, where the surface polarization due to the Maxwell-Wagner effect occurs. The data have been analyzed according to well-established heterogeneous system theories and the passive electrical parameters of both the cytoplasmic and nuclear membranes have been obtained. Moreover, a further analysis to take into account the roughness of the membrane surface on the basis of a fractal model yields new estimates for the membrane conductivity and the membrane permittivity, independently of the surface architecture of the cell. These findings are confirmed by measurements carried out at higher frequencies, in the range from 1 MHz to 1 GHz, on lymphocytes dispersed in both hyperosmotic and hypoosmotic media, that influence the surface complexity of the membrane due to the microvillous protusions. The surface roughness of the cell is described by a macroscopic parameter (the fractal dimension) whose variations are associated to the progressive swelling of the cell, as the osmolality of the solution is changed.

Introduction

In recent years, the study of the passive electrical properties of biomembranes, essentially the permittivity and the conductivity of the cytoplasmic membrane, has gained considerable attention since it might provide an insight into the structure and the functionality of these systems. The use of dielectric measurements for studying the electrical parameters of biological cells or tissues is a well established technique and in the last two decades frequency-domain dielectric spectroscopy in the frequency range from 1 kHz to 100 MHz has been applied in the investigations of a large variety of biological cells and materials of biological relevance and various reviews have appeared [1–4].

These investigations have been applied to cells and biological systems, including cultured lymphoma cells [5], yeast cells [6], *Escherichia coli* [7], human erythrocytes in normal and pathological conditions [8], bacterial chromatophores [9].

The effectiveness of the conductometric method, or more generally of the dielectric methods, in the evaluation of the passive electrical properties of cell membranes is based on the fact that the presence of a low-conductivity layer (the cell membrane) separating two different high-conductivity media (the cytosol and the extracellular medium, in this case) gives rise to a marked conductivity dispersion in the radiowave frequency range, easily evidenced by standard impedance measurements. At a microscopic level, this dispersion is a consequence of a non-uniform charge accumulation at the different interfaces, induced by the applied external electric field, causing an apparent dipole moment whose strength defines the characteristics of the conductivity dispersion, i.e., the conductivity increment and the relaxation time.

The passive electrical parameters, i.e., the membrane conductivity σ and the membrane permittivity ϵ, describe, in principle, both the static and the dynamic behavior of a cell membrane, since these parameters take into account the transport and the permeation processes and moreover the charge arrangement or the polar group distribution on the membrane itself.

* Corresponding author. Fax: +39 6 4463158.

Although extensive investigations on different systems of biological relevance have appeared, comparatively few studies [10–13] have been reported regarding the dielectric and/or conductometric properties of human lymphocytes, which, on the other hand, hold a special interest due to their importance in immunological fields. As an example, a summary of recent data reported in literature on the passive electrical parameters of lymphocyte membranes deduced from dielectric spectroscopy measurements is shown in Table I. The values quoted refer to the conductivities σ_s and σ_n and the permittivities ϵ_s and ϵ_n of the cytoplasmic and nuclear membranes, respectively, and to conductivity of the cytosol σ_p.

The aim of the present work is to undertaken a systematic investigation on the conductometric properties of human lymphocyte membranes in normal and pathological state based on the alterations in the membrane permittivity and membrane conductivity induced by various antitumoral drugs or various physico-chemical agents such as ionizing or non-ionizing radiations or low-molecular-weight ion concentrations. First, however, it is necessary to establish a valid electrical behavior through an accurate evaluation of the passive electrical parameters in human normal resting lymphocytes, under physiological conditions.

To this end, we have measured by means of standard radiowave impedance technique the electrical conductivity of lymphocyte suspensions in the frequency range from 10 kHz to 100 MHz, where the interfacial polarization effects occur. The data have been accurately analyzed with two different dielectric models and the passive electrical parameters describing the electrical behavior of the cell membrane appropriately derived.

The first model is based on the usual dielectric model of a cell suspension, consisting of a collection of particles of appropriate geometry, uniformly dispersed in a continuous medium. The second model considers a more complex cell structure consisting into two different comparts disjoined by different membranes. In this way, the influence of the nuclear membrane inside the cell volume can be appropriately observed. Finally, a somewhat different, but more general, approach to take the lymphocyte membrane surface complexity into account is based on the assumption that the membrane could be, on average, self-similar [14], i.e., its structural organization might possess the same average geometrical construction, but on different size scales. This description should take into account the highly complex surface structure of the cell membrane, independently of the particular details of its architecture.

The role of self-similarity in heterogeneous systems [15] has been investigated by different authors and the fractal analysis has been introduced to describe complex geometries in a variety of biological structures

TABLE I

A summary of recent data reported in literature of passive electrical parameters of lymphocyte membranes deduced from dielectric and conductivity measurements

cells	$\sigma_s(\Omega^{-1}m^{-1})$ [a]	ϵ_s [b]	$\sigma_n(\Omega^{-1}m^{-1})$	ϵ_n	$\sigma_p(\Omega^{-1}m^{-1})$	Ref.
Mouse lymphocytes	$<10^{-6}$	6.8	–	–	0.29	
$R_s = 2.9\ \mu m$						12
$d = 70$ Å						
$\delta = 40$ Å	$<3\cdot10^{-6}$	6.8	$6.0\cdot10^{-3}$	28.0	1.35	
T lymphocytes		4.3				
$d = 50$ Å						
B lymphocytes		16.3				10
$d = 50$ Å						
Lymphocytes		9.8				
$R_s = 3.5\ \mu m$						11
$d = 80$ Å						
Murine lymphocytes		4.6				11
$d = 50$ Å						
T lymphocytes	$(2.7\pm0.5)\cdot10^{-5}$	4.3 ± 03				
$R_s = 2.8\ \mu m$						13
B lymphocytes	$(8\pm1)\cdot10^{-5}$					
$R_s = 2.9\ \mu m$						

[a] Values calculated from $C = \epsilon_0\epsilon_s/d$ where C is the membrane capacitance and ϵ_0 the dielectric constant of free space

[b] Values calculated from $G = \sigma_s/d$ where G is the membrane conductance

such as protein surfaces [16] or synthetic membranes [17].

In the present paper, we have widely analyzed conductometric data of human lymphocyte suspensions obtained from radiowave impedance measurements in the light of the above-stated models, providing a new accurate determination of the passive electrical parameters of cell membrane and we have established upper and lower limits of the conductivity and permittivity of both the cytoplasmic and nuclear membrane.

Experimental

(a) Lymphocyte suspensions in isoosmotic medium. Peripheral blood lymphocytes were collected from healthy donors and sedimented by the Ficoll-Hypaque method and then separated from polymorphonuclear leukocytes by adsorbing the granulocytes on nylon fibers [18].

(b) Lymphocyte suspensions in aniosmotic medium. Additional measurements have been carried out on lymphocytes under aniosmotic conditions, the cells being suspended in both hypoosmotic and hyperosmotic media. The osmolarity of the solution was varied changing the NaCl electrolyte concentration from 65 mmol/l to 190 mmol/l, the isoosmotic osmolarity (which corresponds to 150 mmol/l) being 0.285 osmol/l. The response of lymphocytes in aniosmotic media [19] shows a complex phenomenology. In hypoosmotic medium, the volume of T-lymphocytes first increases owing to the osmotic flow of water molecules through the cell membrane, and then decreases to its initial value, whereas B-lymphpcytes, after the initial volume increase, remain in a swollen state. In hyperosmotic medium, both the T- and B-lymphocytes show a volume decrease without any volume regulation. To investigate the alteration in the electrical parameters induced by aniosmotic media, lymphocytes after staining in isoosmotic saline solution were centrifuged, the supernatant was removed and then the cells were resuspended in the solution of osmolarity appropriate to the volume fraction desired. The electrical conductivity measurements were started after resuspension within 30 min. To verify the effect of aniosmotic media on the dimension and shape of lymphocytes, an accurate investigation was carried out by means of microscopy measurements (see below, Fig. 8).

(c) Scanning electron microscopy. Lymphocytes in solutions of different osmolality were seeded on glass coverslips, pretreated with 0.01% aqueous poly(L-lysine) hydrobromide and allowed to attach for few minutes. The cells were then fixed with 2% glutaraldehyde in 65, 90, 110, 150, 190 mM Millonig buffer, at room temperature, for 20 min. After postfixation with 1% OsO_4 in water for 65, 90, 110 mM and in isotonic Millonig buffer for 150 and 190 mM lymphocytes solutions, the cells were dehydrated through graded ethanol concentrations, critical-point-dried in CO_2 (CPD 010 Balzers device) and golded by sputtering (SCD 040 Balzers device). The samples were then examined with a Stereoscan 360 Cambridge Instrument scanning electron microscope.

(d) Denuted nuclear lymphocyte suspension. Further conductivity measurements have been carried out on lymphocyte nucleus suspensions. Nucleus isolation was performed by following the method used by Koizumi et al. [20] for plasma membrane preparation.

(e) Conductivity measurements in the frequency range 10 kHz to 100 MHz. All conductivity measurements were made using two impedance analyzers Hewlett-Packard model 4192 A (in the frequency range from 10 kHz to 10 MHz) and model 4193 A (in the frequency range from 0.5 MHz to 100 MHz) controlled by a computer as described previously [21]. The measurements were carried out at the temperature of 20.0°C within 0.1°C.

(f) Conductivity measurements in the frequency range 1 MHz to 1G Hz. Additional conductivity measurements were carried out in the frequency range from 1 MHz to 1 GHz by means of an RF Impedance Analyzer (Hewlett-Packard model 4191A). The dielectric cell consisted of a section of a coaxial line with a characteristic impedance of 50 Ω, termined by a standard APC7 connector and directly connected to the meter.

A review of dielectric models of a cell suspension

As stated above, the dielectric models underlying the analysis of dielectric and conductometric measurements of heterogeneous systems have been widely discussed [1–4] and only the most relevant equations will be briefly reviewed here.

(a) 'Single-shell' spherical cell model

The most simple dielectric cell model considers the biological cell suspension as a collection of homogeneous dielectric particles (in this case spheres) of complex conductivity $\sigma_p^* = \sigma_p + i\omega\epsilon_0\epsilon_p$ covered with a thin shell of complex conductivity $\sigma_s^* = \sigma_s + i\omega\epsilon_o\epsilon_s$ which represents the cytoplasmic membrane, randomly dispersed in a continuous medium (the extracellular solution) of complex conductivity $\sigma_m^* = \sigma_m + i\omega\epsilon_o\epsilon_m$. Here σ and ϵ are the conductivity and permittivity of the different media, ω the angular frequency of the applied field, ϵ_o the dielectric constant of free space. The electrical parameters σ and ϵ are assumed to be independent of frequency since, in the present case, our measurements are confined in a frequency interval

up to 100 MHz, well below that of the dipolar relaxation of the aqueous medium, occurring above 10 GHz.

According to the Maxwell-Wagner theory of heterogeneous systems [1] the complex conductivity σ^* of the whole cell suspension is given by

$$\sigma^* = \sigma_m^* \frac{1+2\phi k^*}{1-\phi k^*} \tag{1}$$

with the dipolar factor k^* given by

$$k^* = \frac{\sigma_{eq}^* - \sigma_m^*}{\sigma_{eq}^* + 2\sigma_m^*} \tag{1'}$$

where ϕ is the fractional volume of the dispersed phase and σ_{eq}^* the equivalent conductivity of the particle of radius R_p surrounded by a shell of thickness d

$$\sigma_{eq}^* = \sigma_s^* \frac{\sigma_s^* + \frac{1}{3}(\sigma_p^* - \sigma_s^*)\left[1+2\left(\frac{R_p}{R_p+d}\right)^3\right]}{\sigma_s^* + \frac{1}{3}(\sigma_p^* - \sigma_s^*)\left[1-\left(\frac{R_p}{R_p+d}\right)^3\right]} \tag{2}$$

The general solution of Eqns. 1 and 2 has been described in detail by Pauly and Schwan [22] and by Hanai [23] and predicts the occurrence of two contiguous conductivity dispersions according to a frequency dependence given by

$$\sigma^* = \sigma_m^* \frac{A + i\omega B - \omega^2 C}{D + i\omega E - \omega^2 F}$$

where the full expressions of the quantities *A, B, C, D, E, F*, depending on the electrical parameters of the three different media, are given in detail in Ref. 22. In this model, both the cell membrane and the intramembrane medium (the cytosol) are considered as an homogeneous medium, neglecting any different component and architecture.

(b) 'Double shell' spherical cell model

In this case, owing to the presence in the lymphocyte cell of the nuclear membrane, the cell is modelled with two concentric spheres, each of them bounded by a shell that represents the cytoplasmic membrane (complex conductivity $\sigma_s^* = \sigma_s + i\omega\epsilon_o\epsilon_s$) and the nuclear membrane (complex conductivity $\sigma_n^* = \sigma_n + i\omega\epsilon_o\epsilon_n$). This structure defines two different media, the cytosol of radius R_p with complex conductivity $\sigma_p^* = \sigma_p + i\omega\epsilon_o\epsilon_p$ and an anular region (the intramembrane medium) with complex conductivity $\sigma_i^* = \sigma_i + i\omega\epsilon_o\epsilon_i$. As above, the complex conductivity σ^* of the whole cell suspension is given by Eqn. 1, but, in this case, the equivalent conductivity σ_{eq}^*, that represents of the equivalent conductivity of the effective particle, can be built up by a step by step procedure, considering the different adjacent media, according to the expressions:

$$\sigma_{eq}^* = \sigma_s^* \frac{\sigma_s^* + \frac{1}{3}(\sigma_{eq1}^* - \sigma_s^*)\left[1+2\left(\frac{R_i}{R_s}\right)^3\right]}{\sigma_s^* + \frac{1}{3}(\sigma_{eq1}^* - \sigma_s^*)\left[1-\left(\frac{R_i}{R_s}\right)^3\right]} \tag{3}$$

$$\sigma_{eq1}^* = \sigma_i^* \frac{\sigma_i^* + \frac{1}{3}(\sigma_{eq2}^* - \sigma_i^*)\left[1+2\left(\frac{R_n}{R_i}\right)^3\right]}{\sigma_i^* + \frac{1}{3}(\sigma_{eq2}^* - \sigma_i^*)\left[1-\left(\frac{R_n}{R_i}\right)^3\right]} \tag{3'}$$

$$\sigma_{eq2}^* = \sigma_n^* \frac{\sigma_n^* + \frac{1}{3}(\sigma_n^* - \sigma_p^*)\left[1+2\left(\frac{R_p}{R_n}\right)^3\right]}{\sigma_n^* + \frac{1}{3}(\sigma_n^* - \sigma_p^*)\left[1-\left(\frac{R_p}{R_n}\right)^3\right]} \tag{3''}$$

Here, $d = R_s - R_i$ is the thickness of the cytoplasmic membrane and $\delta = R_n - R_p$ that of the nuclear membrane, where R_n, R_i, R_s are the radius of the nuclear envelope, the external radius of the intramembrane medium and finally the radius of the whole cell.

The 'single-shell' and the 'double-shell' models depend respectively on eight and fourteen different morphological or geometrical parameters involving the different adjacent media. The electrical phase parameters of the external medium (the conductivity σ_m and the dielectric constant ϵ_m) can be measured directly on the supernatant, after centrifuging the suspension. The radius of the whole cell can be determined by optical microscopy measurements and the thickness of both the cytoplasmic and nuclear membranes has been assumed to be $d = \delta = 75$ Å, as usually done. This reduces the number of the free parameters entering into the above two models to four and nine, respectively. It must be noted, however, that the different parameters influence differently [7] the overall conductivity behavior of the suspension.

The Looyenga equation

An alternative expression, which does not involve the shape of the particles and holds especially for high volume faction, has been derived by Looyenga [24]:

$$\sigma^* = \{\sigma_m^{*\frac{1}{3}} + \phi(\sigma_{eq}^{*\frac{1}{3}} - \sigma_m^{*\frac{1}{3}})\}^3 \tag{4}$$

where σ_{eq}^* is the equivalent conductivity of the particle that reduces to Eqn. 2 for the 'single shell' model and to Eqn. 3 for the 'double-shell' model. This equation, originally obtained for a simple two-phase heterogeneous system, gives the whole conductivity behavior of the effective system by substituting the appropriate

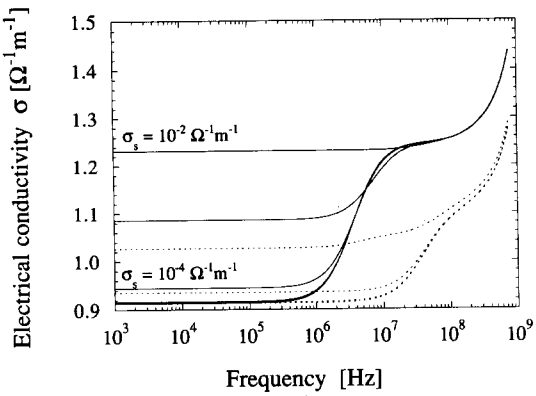

Fig. 1. Typical conductivity dispersions of lymphocyte suspensions in the frequency range from 1 kHz to 1 GHz for different values of the cytoplasmic membrane, according to different dielectric models: (full lines): Maxwell-Wagner theory (Eqn. 1), single-shell model; (dotted lines): Maxwell-Wagner theory (Eqn. 3), double-shell model. The parameters entering Eqns. 1 and 3 are: $\epsilon_s = \epsilon_n = 5$; $\sigma_p = \sigma_i = 0.8$ $\Omega^{-1}m^{-1}$; $\epsilon_p = \epsilon_i = 100$. External radius of the cell $R_s = 5$ μm, thickness of the nuclear and cytoplasmic membrane 75 Å, fractional volume of the dispersed phase $\Phi = 0.30$; conductivity and permittivity of the external medium $\sigma_m = 0.8$ $\Omega^{-1}m^{-1}$, $\epsilon_m = 80$.

expressions of the conductivity of the dispersed particles.

The conductivity dispersions calculated from different dielectric models

Figs. 1 and 2 show the calculated values of the electrical conductivity of a spherical particle suspension in the frequency range from 1 kHz to 1 GHz according to the Maxwell-Wagner theory (Eqns. 1 and 3) and the Looyenga theory (Eqn. 4). Both the single-shell and the double-shell models have been considered. As can be seen, marked conductivity dispersions occur, depending on the values of the different phase parameters involved.

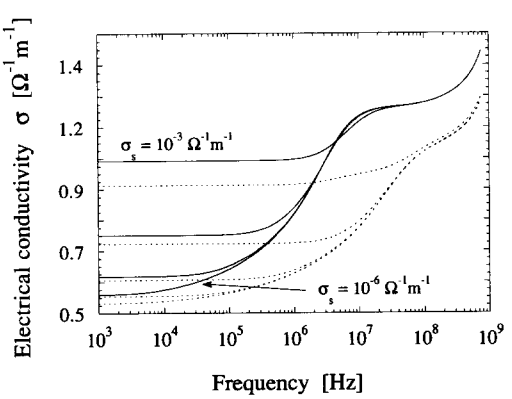

Fig. 2. Typical conductivity dispersions of lymphocyte suspensions in the frequency range from 1 kHz to 1 GHz for different values of the cytoplasmic membrane, according to different dielectric models: (full lines): Looyenga theory (Eqn. 4), single-shell model; (dotted lines): Looyenga theory (Eqn. 4), double-shell model. The values of the phase parameters are shown in the legend of Fig. 1.

The fractal approach

A different attempt to describe a surface structure which shows self-similarity within a certain scaling range is based on a fractal analysis [25,26] that recently has been introduced with great success to take into account complex geometry [14]. This method offers an efficient way of characterizing irregularity in general terms and it has been proven to be extremely useful in a large variety of surface physics and electrochemistry. The main advantage of a fractal approach is that is possible to give a global description of a rough, highly irregular surface by means of a parameter (the fractal dimension D_f) which is insensitive to structural or morphological details. This is particularly true for the cytoplasmic membrane of a lymphocyte cell where the microvilli cause a larger amount of complexity than that observed in other cell surfaces.

Our analysis is based on the assumption that the surface of the lymphocyte membrane behaves similarly to a fractal eletrolyte-electrode interface, i.e., the geometrical property of a rough surface is self-similar under a scale transformation.

Nyikos and Pajkossy [27] and, more recently, De Levie [28] have proposed that the measured interfacial admittance per unit apparent surface obeys a power law

$$Y = by^{\alpha} \tag{5}$$

where $y = G + i\omega C$ is the admittance per unit 'true' surface and b a factor depending on the geometry of the object and on the ionic conductivity of the bathing medium. C and G are the capacitance and the conductance per unit area. The exponent $\alpha = 1/(D_f - 1)$ measures directly the degree of surface irregularity and can be regarded as a measure of the surface roughness, through the fractal dimension D_f. The impedance behavior of rough surfaces is intermediate between that of a planar ($\alpha = 1$, $D_f = 2$) and that of a porous ($\alpha = 1/2$, $D_f = 3$) surface.

Since y refers to the effective true membrane, the capacitance C and the conductance G per unit area can be written as

$$C = \epsilon_0 \epsilon_s / d$$

$$G = \sigma_s / d$$

and consequently the equivalent conductivity of the fractal membrane of apparent thickness d_o is given by

$$\sigma_{sf}^* = d_o\{b(G + i\omega C)^{\alpha}\} \tag{6}$$

In this way, the effective conductivity of a sphere covered by a fractal layer is given by Eqn. 2 or Eqn. 3, according to the single-shell or the double-shell model considered, replacing σ_s^* with Eqn. 6. Following Nyikos

and Pajkossy [29], the coefficient b entering into Eqn. 5 can be generalized to the case of a membrane that encompasses two different media in the form

$$b \sim \left(\frac{1}{\sigma_m} - \frac{1}{\sigma_p}\right)^{\alpha - 1}$$

where σ_m and σ_p are the conductivity of the external and internal medium, respectively.

A brief account of this analysis applied to human lymphocytes has been presented elsewhere [30].

The accuracy of the dielectric models

A final comment is order. Sometimes, it is stressed [31] that, although accurate in the estimate of the membrane capacitance C, these conductivity and/or dielectric methods are unable to provide the value of membrane conductivity owing to its very low value, generally ranging between 10^{-3} and 10^{-5}–10^{-6} Ω^{-1} m^{-1}.

It must be noted, however, that for systems characterized by cells of 1 – 10 μm in diameter and volume fraction sufficiently high ($\Phi = 0.1$ – 0.3), there is sufficient influence of the membrane conductivity σ_s on the overall conductivity of the suspension because it may be properly extracted by means of appropriate fitting procedure. To this end, Fig. 3 shows the total conductivity increment $\Delta\sigma = (\sigma_{inf} - \sigma_0)$, the difference in the limiting values of the conductivity from high to low frequency, as a function of the membrane conductivity σ_s (the conductivity of the cytoplasmic membrane) both for the single-shell and the double-shell model, in a suspension of spherical objects similar to those investigated here. As can be seen, the parameter σ_s is shown to be effective in altering the general shape of the observed conductivity spectra and the conductivity increment is sufficiently large to be properly evaluated and, however, well above the experimental uncertainties, at least for σ_s within the interval 10^{-5} – 10^{-2} Ω^{-1} m^{-1} This means that the model is accurate enough because both the permittivity ε (or in turn the membrane capacitance C) and the membrane conductivity σ (or in turn the membrane conductance G) are determined. It must be noted, however, that suspension methods such as those employed in the present investigation give the average 'macroscopic' value of the whole cell membrane and necessarily consider all the mechanisms involved in the conduction. Other techniques give 'microscopic' values involving a single channel or a specific pore. These values, depending at least in part on the particular ion conduction mechanism, may differ from those derived under different assumptions and may depend on different experimental conditions.

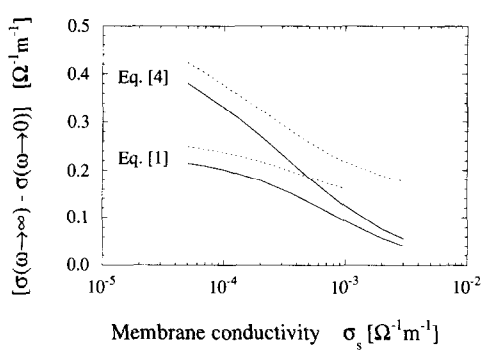

Fig. 3. The influence of the conductivity of the cytoplasmic membrane on the conductivity increment $\Delta\sigma = (\sigma(\omega \to \infty) - \sigma(\omega \to 0))$ according to different dielectric models: (full lines):single shell model; upper curve: Looyenga equation; lower curve: Maxwell-Wagner equation. (dotted lines): double-shell model; upper curve: Looyenga equation; lower curve: Maxwell-Wagner equation. The curves are calculated on the basis of the following parameters: Single-shell: $\epsilon_s = 4$; $\sigma_p = 0.6$ $\Omega^{-1}m^{-1}$. Double-shell: $\epsilon_s = 4$; $\epsilon_i = \epsilon_p = 100$; $\sigma_i = \sigma_p = 0.8$ $\Omega^{-1}m^{-1}$; $\sigma_n = 10^{-3}$ $\Omega^{-1}m^{-1}$ $\epsilon_n = 5$. The extracellular solution is characterized by $\sigma_m = 1.4$ $\Omega^{-1}m^{-1}$ and $\epsilon_m = 80$. The external radius of the cell is $R_s = 3.73$ μm. The thickness of the cytoplasmic and nuclear membrane is assumed to be 75 Å.

Morphology of lymphocyte cells

Since the morphological parameters of the cell have to be known before the analysis of the conductivity spectra can be carried out significantly, the knowledge of the cell shape and cell volume in the effective experimental conditions is required.

During the last decade, various morphometric measurements [32–34] on human lymphocytes have been reported and although a large spread of values has been found, depending on the preparation of the cells and on the technique employed, the reported value for the lymphocyte volume ranges from 180 to 280 μm^3. Recently [35], accurate measurements carried out by means of two different methods, i.e., electronic particle counting and wet weight and density techniques yield a cell volume of (218 ± 4) μm^3 and (203 ± 3) μm^3, respectively.

In the analysis of our measurements we have assumed a cell volume of 217 μm^3, which corresponds to a cell radius of 3.73 μm. Moreover, as is pointed out by Schmid-Schönbein et al. [36], it is well known that lymphocytes possess more membrane surface than that needed to cover a smooth sphere with the mean cell volume. This means that lymphocytes are able to regulate their volume under hypotonic or hypertonic conditions.

Based on light microscopy or scanning and transmission electron microscopy, the general feature which appears is that whereas in hypertonic or isotonic solution (from 600 to 200 mosmol/l) lymphocytes have a folded membrane with many microvilli, in hypotonic media the cell shape changes towards that of a smooth sphere and the average diameter increases from 7.2 μm to about 11 μm at an osmolarity of 100 mosmol/l.

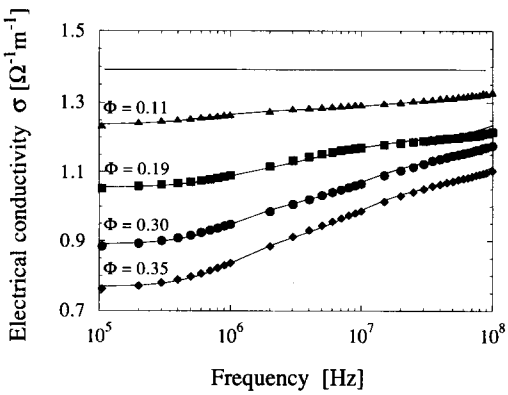

Fig. 4. Some typical electrical conductivity spectra of lymphocyte suspensions in the frequency range from 100 kHz to 100 MHz for various volume fractions F from 0.10 to 0.35 at the temperature of 20.0 ± 0.1°C.

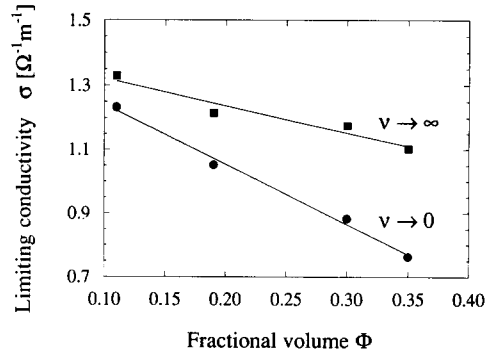

Fig. 5. The dependence of the limiting conductivity values $\sigma_0 = \sigma(\omega \to 0)$ and $\sigma_\infty = \sigma(\mu \to \infty)$ respectively on the volume fraction Φ of the cell suspension.

Results

Typical electrical conductivity spectra of lymphocyte suspensions at some selected cell concentrations, in the frequency range from 1 kHz to 100 MHz are shown in Fig. 4. The data show the usual conductivity dispersion occurring in heterogeneous systems as a consequence of charge accumulation at the boundaries of the different adjacent media, induced by the external electric field.

The conductivity increment (the difference in the limiting values of the conductivity from high to low frequency) and the relaxation time have the typical values observed in cell suspension, where the inner and the outer media (disjoined by the cell membrane) display different dielectric and conductivity properties.

In the present case, we have undertaken an accurate analysis of the experimental data we have obtained on the basis of the different dielectric models described above with the aim to provide a set of electric parameters which can describe the electrical behavior of the cell membranes in human lymphocyte cells.

First of all, we want to verify the linear dependence of the conductivity on the volume fraction Φ. Fig. 5 shows that both the limiting values of the conductivities $\sigma_{inf} = \sigma(\omega \to \infty)$ and $\sigma_0 = \sigma(\omega \to 0)$, vary linearly with Φ up to $\Phi = 0.35$, suggesting that interactions between membranes of adjacent cells should be negligible.

The passive electrical parameters of lymphocyte cells deduced from the traditional heterogeneous mixture equations both for the single- and the double-shell models are shown in Table II. Our analysis is somewhat different from those carried out by different authors [5–7], since the conductivity value of the cytoplasmic membrane is derived directly as a free parameter from the fit of the observed conductivity dispersion, rather than assumed as a fixed value. This procedure seems to be meaningful until the cytoplasmic membrane is able to alter the conductivity behavior of the whole suspension, as shown in Fig. 3.

As stated above, the geometrical and morphological parameters of the cell influence markedly the results.

TABLE II

Passive electrical parameters of lymphocyte cells deduced from different dielectric models

The cell is modeled as a sphere of external radius $R_s = 3.73$ μm and the thickness of the cytoplasmic and nuclear membrane is assumed to be 75 Å. The external radius of the nuclear envelope is 2.85 μm. It corresponds to a nuclear volume 55.4% of the total cell volume. The results are means and standard deviations of ten different experiments.

Dielectric model	$\sigma_s(\Omega^{-1}m^{-1})$ ($\times 10^{-4}$)	ϵ_s	$\sigma_p(\Omega^{-1}m^{-1})$	$\sigma_n(\Omega^{-1}m^{-1})$ ($\times 10^{-3}$)	ϵ_n
Single-shell					
Maxwell-Wagner theory (Eqn. 1)	1.9 ± 0.2	9 ± 1	0.59 ± 0.02	–	–
Looyenga theory (Eqn. 4)	3.7 ± 0.1	5.7 ± 0.4	0.56 ± 0.02	–	–
Double-shell					
Maxwell-Wagner theory (Eqn. 1)	5.6 ± 0.6	21 ± 2	0.41 ± 0.04	2.6 ± 0.7	7 ± 1
Looyenga theory [Eqn. 4]	6.4 ± 0.3	20 ± 2	0.34 ± 0.03	1.7 ± 0.2	5.6 ± 0.9

TABLE III

Passive electrical parameters of lymphocyte nuclei deduced from different dielectric models

The nucleus is modeled as a sphere of external radius 2.85 μm. The thickness of the nuclear membrane is 75 Å. The results are means and standard deviations of ten different experiments.

Dielectric model	$\sigma_n(\Omega^{-1}m^{-1})$ $(\times 10^{-4})$	ϵ_n	$\sigma_p(\Omega^{-1}m^{-1})$
Single-shell			
Maxwell-Wagner theory Eqn. 1	9.2 ± 0.7	14 ± 4	0.25 ± 0.05
Looyenga theory Eqn. 4	8.3 ± 0.5	6.8 ± 0.4	0.32 ± 0.08

To obtain independent information on the nuclear membrane we have performed some additional electrical conductivity measurements on a suspension of denuted nuclei separately obtained from the lymphocyte suspensions following the method of Koizumi [20]. In this case, only the single-shell model holds and the results of the analysis of the data are shown in Table III.

Fig. 6 shows, in some typical cases, a comparison between the single and double-shell models. The electrical parameters of the lymphocyte cells have been determined by fitting the theoretical curves (Eqns. 1 and 3) to the observed conductivity dispersion data to four or nine free parameters, respectively, according to the dielectric model adopted (however, in what follows, we report on the parameters that describe the electrical behavior of the cell membranes and influence markedly the overall conductivity spectrum, i.e., the conductivities σ_s and σ_n, the permittivities ϵ_s and ϵ_n and the conductivity of the cytosol σ_p).

As can be seen, when based on the double-shell model, the fitting improved appreciably, even if the number of the free parameters involved is increased.

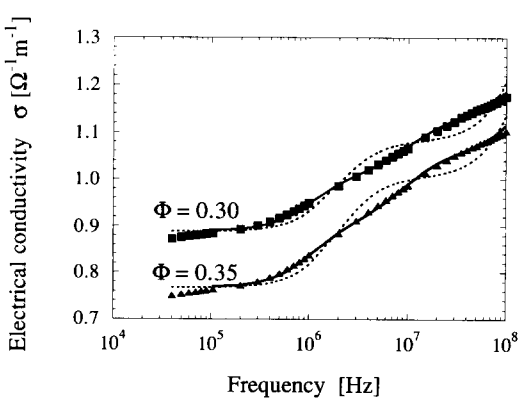

Fig. 6. The conductivity dispersion of lymphocyte suspensions at two different volume fractions Φ in the frequency range from 10 kHz to 100 MHz. The dotted and full lines represent the calculated values according to the Maxwell-Wagner theory with the single- and the double-shell model, respectively.

As can be seen in Fig. 6, the conductivity dispersions extend over a wide frequency range and the occurrence of the multiple relaxation process is probably due, in the present case, to the complex structure of the lymphocyte cells which comprises, at least, two different regions, i.e., the inner medium (the cytosol) and a intramembranous medium, between the nuclear and cytoplasmic membrane. These indications provide further evidences for an analysis of the conductivity measurements based on the double-shell model. The most relevant findings can be summarized as follows.

(i) The conductivity of the cytoplasmic membrane ($\sigma_s = (5.6 \pm 0.6)\ 10^{-4}\ \Omega^{-1}\ m^{-1}$) is considerably lower than the conductivity of the nuclear membrane ($\sigma_n = (2.6 \pm 0.7)\ 10^{-3}\ \Omega^{-1}\ m^{-1}$). This means that the transmembrane permeation is more active across the nuclear membrane.

(ii) The permittivity of the cytoplasmic membrane ($\epsilon_s = 21 \pm 2$) is higher than that of the nuclear membrane ($\epsilon_n = 2.6 \pm 0.7$). The nuclear membrane possesses a lower content of membrane proteins and other transmembranous components which reflects in a lower dielectric constant, very similar to that of a simple lipid bilayer.

(iii) The double-shell model based on the Maxwell-Wagner equation or on the Looyenga equation substantially furnishes the same values for the membrane electrical parameters. This circumstance suggests that the mean field approximations, upon which the two theories hold, are in the present case verified. The values shown in Table II are a somewhat higher than those derived by other authors in a variety of different cells [5–7] on the basis of a different fitting procedure. However, a very rough determination of the cytoplasmic membrane conductivity σ_s can be obtained considering the transport across the membrane as due to the existence of conducting pathways embedded in the hydrocarbon bilayer. If the pore density, N_p, of the human lymphocyte membrane is of the order of 10^{11} pore/m^2 and each pore, having a diameter, D, of about 9 nm and a length of about 80 nm, contains an aqueous solution of conductivity 1–2 $\Omega^{-1}m^{-1}$, the membrane conductivity can be written, to a first approximation, as

$$\sigma_s = N_p \sigma_p \pi \left(\frac{D}{2}\right)^2$$

With the values quoted above, this equation yields a value of $\sigma_s = 10^{-5}\ \Omega^{-1}m^{-1}$, of the same order of magnitude than that derived from our conductivity measurements.

(iv) When the parameters of the nuclear membrane are derived directly from measurements carried out on a suspension of nuclei, somewhat higher values are obtained, in comparison with those derived from the

double-shell model on intact lymphocyte suspensions. In reality, the complex structure of these cells makes the separation of the cytoplasmic membrane from the adjacent surrounding media difficult and this process may alter some properties of the nuclear membrane. A physical link between the cytoplasmic membrane and the nuclear envelope has been recently suggested by Hoekstra et al. [21]. In other words, the nuclear membrane, isolated from the remaining components of the lymphocyte cell, may behave differently and the electrical parameters estimated in these conditions may refer to the nuclear membrane and its immediate neighboring. In this case, values more similar to those derived for the cytoplasmic membrane are expected. Nevertheless, the data agree well within one order of magnitude and this finding is a further support for the effectiveness of the analysis based on the double-shell model.

As pointed out by Davey at al. [37], the irregular surface morphology of many biological cells can give rise to a significant overestimation of the membrane electrical parameters, suggesting that the models described earlier are less than adequate for cells exhibiting a marked degree of microvillosity. The lymphocyte surface is rough, due to the existence of many microvillous projections extending towards the extracellular solution. On the other hand, the above models consider the membrane as a homogeneous medium characterized by a bulk permittivity and a bulk conductivity and parameters obtained from this method must be considered as 'effective' values, characterizing the average properties of the medium.

The 'fractal' approach we propose overcame these difficulties. The results of this analysis derived from the Maxwell-Wagner and the Looyenga theory (Eqn. 1 and Eqn. 4, respectively, are shown in Table IV. Fig. 7 shows the calculated values of the conductivity of lymphocyte suspensions at some selected concentrations according to the fractal theory (Eqns. 5 and 6), using both the Maxwell-Wagner and the Looyenga models. Here, we have confined this analysis to the single-shell model, since the fractal behavior should affect the cytoplasmic membrane only. The parameters involved, besides the membrane permittivity ϵ_s and the membrane conductivity σ_s, are the exponent a which defines the fractal dimension D_f and the parameter d_0 which gives the extension where the fractal-like properties of the membrane occurs.

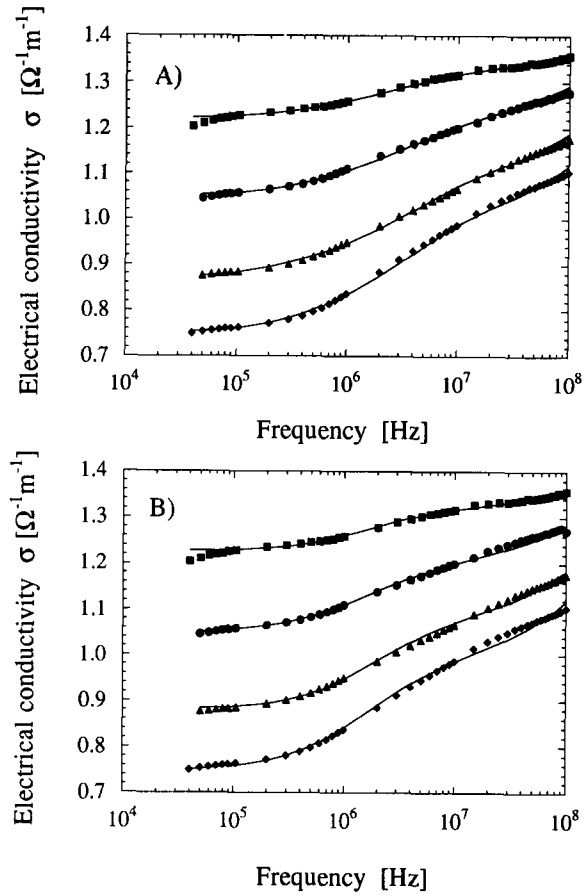

Fig. 7. The electrical conductivity dispersion in lymphocyte suspensions in the frequency range from 10 kHz to 100 MHz at different volume fractions Φ. (A) Looyenga theory (Eqn. 4); (B) Maxwell-Wagner theory (Eqn. 1) (■) $\Phi = 0.13$; (●) $\Phi = 0.22$; (▲) $\Phi = 0.30$; (◆) $\Phi = 0.35$. The full lines in both the plots represent the calculated values according to the fractal description of the surface roughness, within the single-shell model.

As can be seen in Table IV, the membrane conductivity σ_s assumes values of the order of magnitude of $(3\text{–}4) \cdot 10^{-5}\ \Omega^{-1}\ m^{-1}$, well different from those de-

TABLE IV

Passive electrical parameters of cytoplasmic membrane of lymphocyte cells deduced from different dielectric mixture equations on the basis of the fractal analysis of the data

The results are means and standard deviations of ten different experiments.

Dielectric model	$\sigma_s(\Omega^{-1}m^{-1})$ $(\times 10^{-5})$	ϵ_s	$\sigma_p(\Omega^{-1}m^{-1})$	D_f	$d_0(\mu m)$
Single-shell					
Maxwell-Wagner theory (Eqn. 1)	5.7±0.2	19.2±0.4	0.59±0.03	2.30±0.09	0.74±0.07
Looyenga theory (Eqn. 4)	3.4±0.7	4.7±0.2	0.33±0.03	2.14±0.05	1.10±0.04

rived from the usual analysis of the data. Moreover, the parameter d_0 assumes a value of the order of 1 μm, in very good agreement with the thickness of the microvillous protrusions observed by microscopy.

It is noteworthy that the exponent α is intermediate between that of a planar surface ($\alpha = 1$) and that of a porous surface ($\alpha = 1/2$), indicating that the lymphocyte membrane surface does not fill uniformly a two-dimensional space, but rather extends in the external solution. The fractal dimension is $D_f = 2.14 \pm 0.05$.

The fractal characterization of the membrane surface, according to the model proposed by Nyikos and Pajkossy [27] and by De Levie [28], tells us that the phase electrical parameters deduced from radiowave impedance measurements assume values different from those estimated in the usual way.

To investigate further the conductometric properties of the lymphocyte membranes and moreover to evaluate the effectiveness of the fractal approach in describing the high complexity of their surface, we have carried out a set of conductivity measurements with lymphocyte cells equilibrated in aniosmotic solutions of appropriate osmolarity, between 100 to 500 mosmol/l, in order to obtain changes in the cell volume in a controlled way, with a consequent modification of the surface to volume ratio.

Recent measurements [36] have shown that below 250 mosmol/l the lymphocyte cells swell markedly, the average diameter changing from 7.46 μm in isotonic solution, to 10.1 μm or more in hypotonic solution. This swelling should be accompanied by a progressive reduction of the surface roughness of the cell with a consequent decrease of the fractal behavior.

Fig. 8 shows the surface of different lymphocyte cells dispersed in aniosmotic solution obtained from scanning electron microscopy. As can be seen, when dispersed in hypotonic solution, the surface roughness is strongly reduced and the cell assumes a more marked smooth surface.

These further conductivity measurements have been carried out in the frequency range from 1 MHz to 1 GHz, in a frequency interval higher than that previously investigated. The main advantage of this strategy is that, with our experimental set-up, each measurement requires less that 50 μl of sample volume allowing that at least five or six different runs can be investigated starting from the same sample preparation. In this way it is possible to change the osmolarity of the solution in a larger number of samples starting from the same lymphocyte cells, without introducing some possible ambiguities due to any different characteristic of lymphocytes obtained from different donors.

On the other hand, at higher frequencies, a further conductivity dispersion occurs, due to the orientational polarization effect of the water phase. This circumstance contributes to make the conductivity spectra more complicated and, as a consequence, the electrical parameters of the cell membranes must be extracted from a more complex dielectric model.

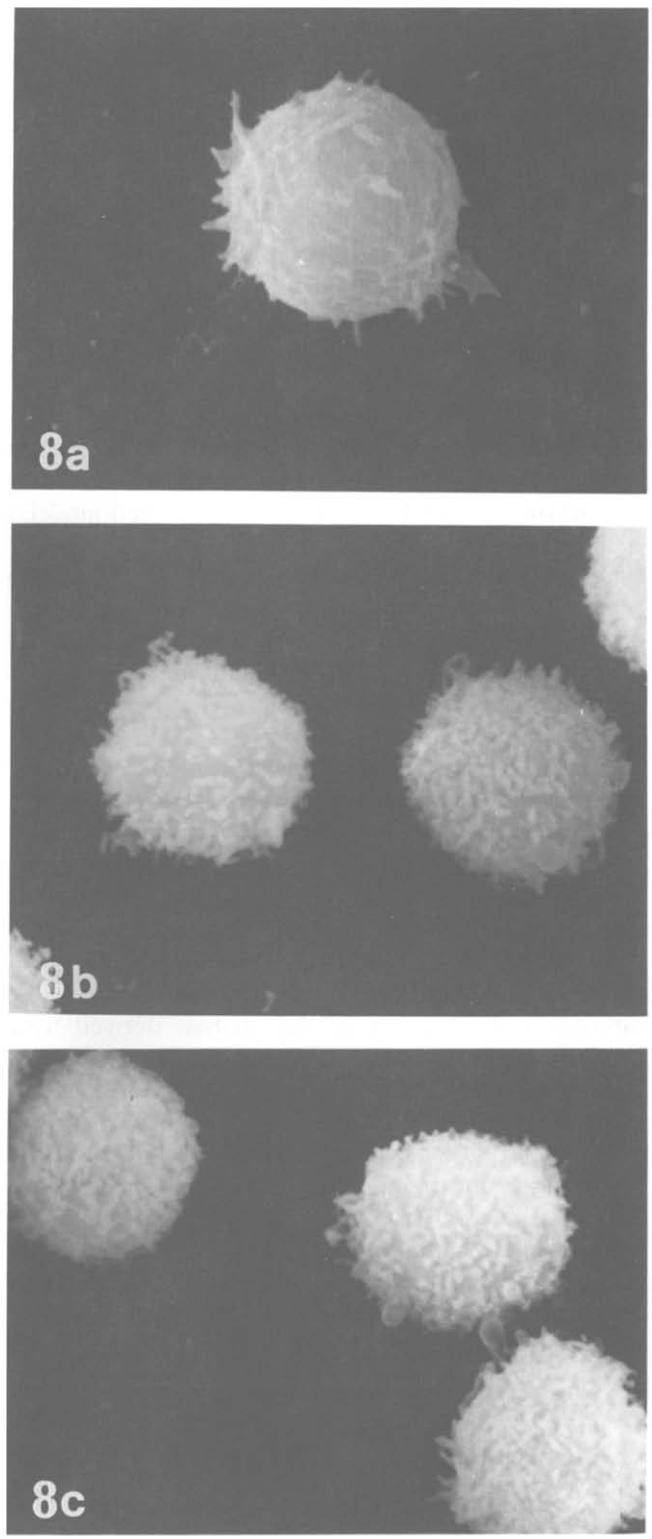

Fig. 8. Scanning electron microscopy images of lymphocyte cells when dispersed in aniosmotic media obtained varying the NaCl electrolyte concentration: (a) 65 nmol/l; (b) 150 mmol/l; (c) 190 mmol/l.

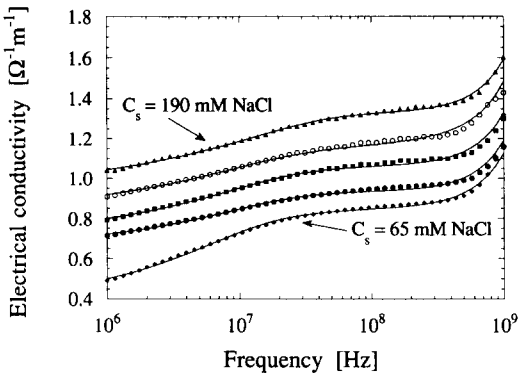

Fig. 9. The electrical conductivity of lymphocytes dispersed in saline solutions of different osmolarity as a function of frequency, in the range 1 MHz to 1 GHz. The volume fraction is $\Phi = 0.20$. The osmolarity of the solution is varied changing the NaCl concentration: (▲) 190 mM, (○) 150 mM, (■) 110 mM, (●) 90 mM, (◆) 65 mM. The full lines represent the calculated values according to the fractal theory within the Looyenga model to which a further dispersion characterized by a Deybe-type relaxation function has been added to take into account the dispersion occurring in the aqueous phase at higher frequencies.

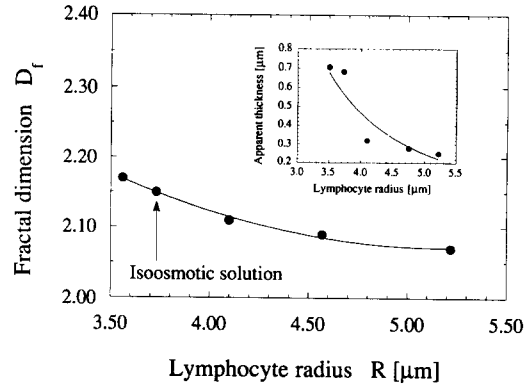

Fig. 10. The fractal dimension D_f as a function of the lymphocyte radius derived from fractal theory within the Looyenga model. The inset shows the concomitant decrease of the thickness of the surface layer when the 'fractal' behavior holds.

Typical conductivity spectra of lymphocytes suspended in aniosmotic solutions in the frequency range from 1 MHz to 1 GHz are shown in Fig. 9. As can be seen, the marked increase in the conductivity in the high-frequency region is due to the aqueous phase relaxation. The data have been analyzed on the basis of the dielectric models described above, where a further conductivity dispersion modeled with a Deybe-type function has been added. Here, the comparison is confined within the single-shell model only in both the Maxwell-Wagner or Looyenga theory and in the fractal theory. Table V furnishes the values of the relevant parameters of the cytoplasmic membrane when the NaCl electrolyte concentration has been changed from 65 to 190 mmol/l.

The main findings concern with the progressive increase of the exponent a as the osmolarity of the solution decreases accompanied by a consequent reduction of the apparent thickness d_0 of cytoplasmic membrane.

To sum up the consideration of the data presented above, we can say that, as far as the usual analysis is concerned, the double-shell model provides a very good description of the conductivity behavior of lymphocyte cell suspensions over a wide frequency range. In this context, the Looyenga equation appear to work in a satisfactory way also at high concentration of the dispersed cells.

As far as the fractal analysis we proposed is concerned, two interesting findings must be considered, i.e., the fractal dimension D_f tends to the expected values for a smooth surface as the lymphocyte volume is increased after the cells are dispersed in hypotonic solution. As D_f tends towards 2, there is a concomitant decrease of the apparent thickness of the cytoplasmic membrane layer where the microvillous structure exists and where the fractal analysis holds. Fig. 10 shows the progressive decrease of the fractal dimension D_f as the lymphocyte radius is increased as a consequence of the aniosmotic treatment. The concomitant decrease of the apparent thickness of the 'fractal' membrane layer is shown in the inset of Fig. 10. This finding provides evidence that the fractal analysis considered so far should furnish, on the basis of a relatively simple

TABLE V

The passive electrical parameters of the cytoplasmic membrane of lymphocyte cells dispersed in aniosmatic solutions of different osmolality

The parameters have been derived from a non-linear least squares fitt to Eqns. 1 and 4 (the Maxwell-Wagner and Looyenga theories) or to Eqns. 5 and 6 (the fractal model).

Lymphocyte cells ($\Phi = 0.20$)			Maxwell-Wagner theory		Looyenga theory		Fractal theory			
NaCl (mmol/l)	Π(mosmol/l)	$R_s(\mu m)$	$\sigma_s(\Omega^{-1}m^{-1})$	$\epsilon_s(\Omega^{-1}m^{-1})$	$\sigma_s(\Omega^{-1}m^{-1})$	$\epsilon_s(\Omega^{-1}m^{-1})$	$\sigma_s(\Omega^{-1}m^{-1})$	$\epsilon_s(\Omega^{-1}m^{-1})$	α	$d_0(\mu m)$
65	100	5.22	$1.10 \cdot 10^{-4}$	2.49	$2.00 \cdot 10^{-5}$	2.69	$2.5 \cdot 10^{-5}$	4.26	0.922	0.32
90	154	4.54	$1.05 \cdot 10^{-4}$	2.70	$2.44 \cdot 10^{-4}$	2.05	$3.40 \cdot 10^{-5}$	4.26	0.914	0.278
110	198	4.10	$1.03 \cdot 10^{-4}$	2.46	$2.64 \cdot 10^{-4}$	2.25	$3.40 \cdot 10^{-5}$	4.22	0.902	0.320
150	285	3.73	$1.60 \cdot 10^{-4}$	2.90	$2.81 \cdot 10^{-4}$	2.48	$3.40 \cdot 10^{-5}$	4.26	0.870	0.692
190	375	3.56	$5.34 \cdot 10^{-4}$	4.25	$5.38 \cdot 10^{-4}$	3.58	$4.89 \cdot 10^{-5}$	8.04	0.839	0.706

geometry, a set of electrical phase parameters that are significant.

These parameters that are considerably different for those derived on the basis of more traditional models, are, to a first approximation, independent of the shape and complexity of the membranous surface and should be the 'true' values of the lymphocyte membrane.

References

1 Foster, K.R. and Schwan, H.P. (1986) in CRC Handbook of Biological Effects of Electromagnetic Fields (Polk, C. and Postow, eds.), pp. 27–96, CRC Press, Boca Raton.
2 Pethig, R. and Kell, D.B. (1987) Phys. Med. Biol. 32, 933.
3 Takashima, S. (1989) Electrical Properties of Biopolymes and Membranes, Adam Hilger, Bristol.
4 Kell, D.B. and Harris, C.M. (1985) J. Bioelectr. 4, 317.
5 Irimajiri, A., Doida, Y., Hanai, T. and Inouye, A. (1978) J. Membr. Biol. 38, 209.
6 Asami, K., Hanai, T. and Koizumi, N. (1976) J. Memb. Biol. 28, 169.
7 Asami, K., Hanai, T. and Koizumi, N. (1980) Biophys. J. 31, 215.
8 Ballario, C., Bonincontro, A., Cametti, C., Rosi, A. and Sportelli, L. (1984) Z. Naturforsch 39c, 160, 1163
9 Kell, D.B. (1983) Bioelectrochem. Bioenerg. 11, 405.
10 Surowiec, A., Stuchly, S.S. and Izaguirre, C. (1986) Phys. Med. Biol. 31, 43.
11 Jaroszynski, W., Terlecki, J. and Sulocki, J. (1985) Studia Biophys. 107, 117.
12 Asami, K., Takahashi, Y. and Takashima, S. (1989) Biochim. Biophys. Acta 1010, 49.
13 Hu, X., Arnold, W.M. and Zimmermann, U. (1990) Biochim. Biophys. Acta 1021, 191.
14 Avnir, D. (ed.) (1989) The fractal approach to heterogeneous chemistry, John Wiley & Sons, New York.
15 Dissado, L.A. (1990) Phys. Med. Biol. 35, 1487.
16 Goetze, T. and Brickmann, J. (1992) Biophys. J. 61, 109.
17 Tam, C.M., Matsuura, T. and Tremblay, A.Y. (1991) J. Colloid Interface Sci. 147, 206.
18 Berger, S.L. (1979) Methods Enzymol. 58, 486–494.
19 Hoekstra, A.G., Aten, J.A. and Sloot, P.M.A. (1991) Biophys. J. 59, 765.
20 Koizumi, K., S. Shimizu. Koizumi, K.T., Nishida, K., Sato, C., Ota, K. and Yomonaka, N. (1981) Biochim. Biophys. Acta 649, 393.
21 Diociauti, M., Molinari, A., Calcabrini, A., Arancia, G., Isacchi, G., Bordi, F. and Cametti, C. (1991) Bioelectrochem. Bioenerg. 26, 177.
22 Pauly, H. and Schwan, H.P. (1959) Z. Naturforsch 14b, 125.
23 Hanai, T. (1968) in Emulsion Science (Sherman, P., ed.), p. 353, Academic Press, New York.
24 Looyenga, H. (1965) Physica 31, 401.
25 Mandelbrot, R. (1982) The fractal geometry of nature, Freeman, San Francisco.
26 Pietronero, L. and Tosatti, E. (eds.) (1986) Fractals in Physics. Proocedings of the Sixth Trieste International Symposium of Fractals in Physics, North-Holland, Amsterdam.
27 Nyikos, L. and Pajkossy, T. (1985) Electrochim. Acta 30, 1533.
28 De Levie, R. (1989) J. Electroanal. Chem. 261, 1.
29 Nyikos, L. and Pajkossy, T. (1989) Electrochim. Acta 34, 171, (1989); 34, 181.
30 Bordi, F., Cametti, C. and Di Biasio, A. (1990) Biochim. Biophys. Acta, 1028, 201.
31 Takashima, S., Asami, K. and Takahashi, Y. (1988) Biophys. J. 54, 955.
32 S. Ben-Sasson, Patinkin, D., Grover, N.B. and Doljanski, F. (1974) J. Cell Physiol. 84, 205.
33 Hempling, H.G. (1977) Acta Cytol. 21, 96.
34 Braylan, R.C., Fowlkes, B.J., Jaffe, E.S., Sanders, S.K., Berard, C.W. and Herman, C.J. (1978) Cancer 41, 201.
35 Segel, G.B., Cokelet, G.R. and Lichtman, M.A. (1981) Blood 57, 894.
36 G.W. Schmid-Schönbein, Shih, Y.Y. and Chien, S. (1980) Blood 56, 866.
37 Davey, C.L., Kell, D.B. and Kemp, R.B. (1988) Bioelectrochem. Bioenerg. 20, 83.